

# Computer simulation of fluid phase transitions

Nigel B. Wilding

*Department of Mathematical Sciences, The University of Liverpool,  
Liverpool L69 7BZ, U.K.*

The task of accurately locating fluid phase boundaries by means of computer simulation is hampered by problems associated with sampling both coexisting phases in a single simulation run. We explain the physical background to these problems and describe how they can be tackled using a synthesis of biased Monte Carlo sampling and histogram extrapolation methods, married to a standard fluid simulation algorithm. It is demonstrated that the combined approach provides a powerful method for tracing fluid phase boundaries.

## I. INTRODUCTION

One of the fundamental tasks of statistical mechanics is to forge the link between the *microscopic* (atomic-scale) description of a particular substance and its equilibrium *macroscopic* (thermodynamic) properties. Typically the former is prescribed in terms of a *model*, ie. a specification of the constituent molecules and their mutual interactions. Given this, the challenge is to derive the associated macroscopic properties —quantities such as the compressibility, heat capacity and, above all, the phase behaviour i.e. the conditions under which the substance forms a solid, liquid or gas. Computer simulation allows one to do this.

In many respects, a simulation can be viewed as an experiment performed not on a real substance, but on a model system stored in a computer's memory. As in real experiments, one has to prepare a properly equilibrated sample under the desired thermodynamic conditions; and, just as in real experiments, one can measure the physical properties of that substance, perhaps leading to new discoveries as a result! But, a simulation can have important advantages over a real experiment. Since one is dealing with a numerical model, substances can be studied that are too expensive, too complicated or too dangerous to be tackled by real experiment. Furthermore, since the simulator has access to full and complete information about the state of the simulated system, there are fewer restrictions on just which properties can be measured. Accordingly, information and insight can be gleaned from a simulation which would not readily be obtainable by experimental means [1].

However simulations do have their limitations. The chief drawbacks are constraints on computer speed and memory; most contemporary computers can deal only with systems comprising a few thousand particles —many orders of magnitude fewer than the  $\sim 10^{23}$  typically found in experimental samples. Such restrictions engender so-called finite-size effects in the results, ie. spurious artifacts and systematic discrepancies (compared to the bulk limit) the magnitude of which need to be quantified. It should also be borne in mind that irrespective of the sophistication of the simulation techniques employed, results for macroscopic equilibrium behaviour will reflect

reality only to the extent that the underlying model correctly captures the true microscopic nature of the substance under study. As the old computing adage goes: rubbish in, rubbish out.

Simulation strategies for obtaining the equilibrium phase behaviour of classical fluid systems come in a profusion of different shapes and forms, but broadly speaking fall into two main categories: Molecular Dynamics (MD) and Monte Carlo (MC). Both have been previously discussed extensively in a number of introductory texts and articles, see eg. refs. [2–5]. The MD approach involves computing the phase space trajectories of a system of mutually interacting particles by integrating Newton's equations of motions through time. Physical properties are measured in terms of configurational or time averages as the simulation evolves. MD represents an attractive method in situations where one is interested in obtaining dynamical information about a system, and can also be employed to obtain single phase thermodynamical properties. However for studies of phase transitions, ie. the process by which one phase spontaneously transforms into another, it is rarely a suitable approach because of the problem of hysteresis (superheating and supercooling) wherein the temperature and pressure at which the transition occurs in a simulation may differ significantly from that of the bulk system. This matter is described in detail in sec. II.

Phase transitions (it now seems quite generally agreed) are best tackled by Monte Carlo (MC) simulation. Here one employs a stochastic Markov process to generate a sequence of equilibrium configurations of the model system of interest; physical properties are measured as configurational averages over the sequence [2–5]. The actual mechanisms by which the system evolves from one equilibrium configuration to the next are essentially *artificial*, so information about physical dynamical processes is strictly limited. Nevertheless this loss is compensated for by potential gains in a variety of other areas. Specifically, freed from the strictures imposed by physical dynamics, the simulator is at liberty to construct any number of elaborate schemes via which the simulation efficiently explores the space of possible model configurations. By so doing it becomes possible to bridge time and length scales which

cannot be probed using MD.

In this article we shall focus on one area in which recently developed MC simulation techniques allow one to circumvent an old problem, namely that of accurately obtaining the phase behaviour of model fluids. The approach we describe is in essence a synthesis of a number of existing simulation techniques (developed originally in the context of lattice spin models) which, when married with a standard grand canonical or constant pressure ensemble fluid simulation, provide a powerful and efficient route to phase coexistence properties. Before embarking on this description, however, it is instructive to review some key aspects of phase transition phenomenology, in particular the origins of the hysteresis effect which for many years plagued simulation studies of phase transition and which necessitated the new methodological advances.

## II. HYSTERESIS, INTERFACES AND THE FREE ENERGY BARRIER

The phase diagram of a typical simple substance such as Argon, is depicted in schematic form in figure 1. Depending on the imposed conditions of temperature and pressure, the substance can exist in three phases: solid, liquid or gas. The corresponding regions of the phase diagram are delineated by phase boundaries at which transitions occur from one phase to another. Notable features of this phase diagram are the triple point where three phase boundary lines meet and the liquid-gas critical point which terminates the liquid-gas phase boundary and beyond which all distinction between the liquid and the gas vanishes.

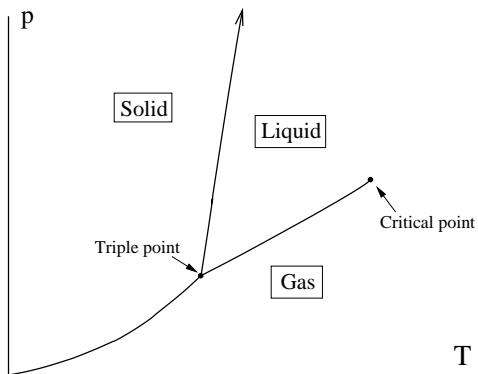


FIG. 1. Phase diagram of a simple substance in the pressure–temperature plane.

Phase diagrams such as that of fig. 1 can be interpreted within the framework of thermodynamics by appeal to the concept of free energy. A system in equilibrium will always choose its state to be that for which the free energy is least [6]. Phase boundaries then arise naturally as that sets of points in the phase diagram for which

two phases have the same free energies, being equally favoured thermodynamically. In experiments, however, a transition from one stable phase to another will not always occur exactly on the phase boundary. Instead one generally encounters ‘overshoot’ or ‘hysteresis’, whereby the actual transition point depends on the thermodynamic history of the sample.

The following *gedanken* experiment will help to explain the origin of hysteresis. Imagine we take a purified quantity of a fluid such as water, place it in a sealed piston-cylinder arrangement at constant atmospheric pressure, and heat it up very slowly so that it always remains close to equilibrium. During this process, the water temperature will rise until at some point it boils –transforming into steam with a concomitant large and abrupt increase in the system volume. This is an example of what is called a first order phase transition. If, however, we stop adding heat before all the water has vapourised we observe *coexistence* between the liquid and vapour phases i.e. a portion of the container will be occupied by the liquid phase, separated by an interface from the remainder which contains vapour (cf. fig. 2). In transforming from one phase to another, a system always passes through such mixed-phase configurations and it is these that are responsible for hysteresis.

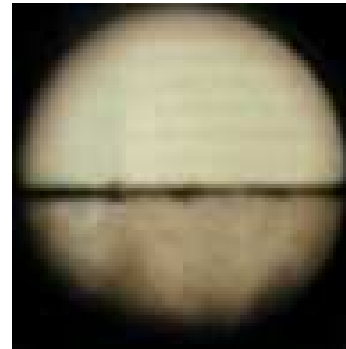


FIG. 2. Photograph of coexisting liquid water and steam in a closed container. The denser liquid occupies the lower portion of the container, separated by an interface from the vapour.

It transpires that mixed-phase configurations possess a higher free energy than pure phase states and since this additional free energy is wholly associated with the interface itself, it is often referred to as the *surface tension*. Owing to their surface tension, mixed-phase configurations are thermodynamically less favourable than pure phase states at the phase boundary. This has a bearing on phase transitions such as the vaporisation of our water sample. As the water is slowly heated it eventually attains the phase boundary temperature  $T = 373.15$  K above which steam has a lower free energy than liquid water i.e. becomes the thermodynamically favoured state. Nevertheless it is possible to ‘superheat’ liquid water some way beyond this temperature without it trans-

forming to steam because, in order to do so, it must pass through the mixed-phase states of higher free energy. A similar effect occurs when cooling steam –it becomes possible to ‘supercool’ it some way below 373.15 K without it liquefying. Hence the temperature at which the transition occurs is not that at which the free energies of the two phases are equal, but instead depends on the initial state of the sample and the direction and rate in which the boundary is traversed.

Much the same thing occurs in simulations of first order phase transitions. But here the problem is also intimately bound up with issues of finite-size effects and simulation timescales. To appreciate how a simulation behaves near a first order phase transition, it is instructive to consider a concrete example, namely the liquid-gas transition of a prototype model fluid –the famous Lennard-Jones fluid (LJF). Within this model, the interaction potential for two point particles separated by linear distance  $r$  is given by

$$U(r) = 4\epsilon \left( \left( \frac{\sigma}{r} \right)^{12} - \left( \frac{\sigma}{r} \right)^6 \right)$$

where the parameters  $\epsilon$  and  $\sigma$  set the strength of the interaction and the length scale respectively [2].

One way of performing a MC simulation of the LJF is to employ the grand-canonical ensemble (GCE) in which, for a given system volume  $V$ , the total configurational energy  $E$  and particle number  $N$  are permitted to fluctuate stochastically, but with average values determined by prescribed values of the temperature  $T$  and chemical potential  $\mu$ . These latter two variables span the phase diagram and by tuning their values, transitions can be induced between gas, liquid and solid phases (cf. fig. 1).

An outline of the operation of a GCE MC simulation is given in box 1. Fluctuations in the energy and particle number occur by means of particle insertions and deletions. MC updates consist of either an insertion or a deletion attempt, each of which is proposed with equal probability. For an insertion, one chooses a random position in the simulation box and calculates the energy change  $\Delta E^I$  associated with placing a new particle at that position. The trial insertion is accepted with a probability given by a so-called Metropolis rule designed to ensure that detailed balance is maintained –a necessary condition for attaining thermodynamic equilibrium [2]:

$$p_{\text{acc}}(N \rightarrow N + 1) = \min \left[ 1, \frac{zV}{(N + 1)} \exp(-\beta(\Delta E^I)) \right] \quad (2.1)$$

where  $z = \exp(\beta\mu)$  with  $\beta = 1/k_B T$ .

Similarly for a particle deletion, one chooses a particle at random from those currently present in the system, calculates the energy change  $\Delta E^D$  associated with its removal and then performs the removal with a probability again given by a Metropolis rule

$$p_{\text{acc}}(N \rightarrow N - 1) = \min \left[ 1, \frac{N}{zV} \exp(-\beta(\Delta E^D)) \right] \quad (2.2)$$

The function rand() generates a random number uniform in [0,1].  
The subroutine ENER() calculates the energy of a particle at a given position.

SUBROUTINE GCEMC

```

IF (RAND().GT.0.5) THEN                                Choose deletion or insertion with
IF(N.LE.0) RETURN                                     equal probability
PD=1+INT (RAND()*N)                                  Select a particle for deletion
DE=ENER(X(PD))                                        Energy of particle
PROB=N*EXP(BETA*DE)/(Z*V)                             Metropolis acceptance probability
IF (RAND().LT.PROB) THEN
  X(PD)=X(N)                                           Accepted: remove particle
  N=N1
ENDIF
ELSE
XI = RAND()*L                                          New particle at random position
DE=ENER(XI)                                             Energy of new particle
PROB=Z*V*EXP(BETA*DE)/(N+1)                           Metropolis acceptance probability
IF (RAND().LT.PROB) THEN
  X(N+1)                                               Accepted: add new particle
  N=N+1
ENDIF
ENDIF
RETURN
END

```

**Box 1:** Outline operation of a simple GCE simulation program. For brevity only the operations for the  $x$  coordinate of particle position vector has been given. Analogous operations apply to the  $y$  and  $z$  coordinates.

Notwithstanding its simplicity, a GCE simulation of this type can provide a highly efficient computational route to equilibrium fluid phase properties. This is especially so if, as is customary, the interparticle potential  $U(r)$  is truncated at some cutoff radius  $r_c$  [2]. Contributions to  $\Delta E^I$  and  $\Delta E^D$  then arise only via local interactions and, by partitioning the simulation box into cubic cells of side  $r_c$ , the subset of contributing particles can be readily identified. Note also, that for studies of liquid-gas phase transitions one gains nothing by implementing explicit particle displacement moves in a GCE simulation. Instead these are realized *implicitly* by virtue of repeated particle transfers, sole use of which not only constitutes a valid algorithm (it is clearly ergodic) but, moreover, focuses the computational effort on the bottleneck for phase space evolution namely the fluctuations in the particle number density.

Let us now examine how the GCE simulation algorithm of Box 1 behaves in the vicinity of the liquid-gas phase boundary. The primary observables of interest from such a simulation are the particle number  $N$  and the configurational energy  $E(\{\mathbf{r}\})$  where  $\{\mathbf{r}\}$  denotes the set of particle position vectors i.e. the configuration. The fluctuations of the particle number density,  $\rho = N/V$ , in particular provide much insight into the nature of phase coexistence in a finite-sized system. In a simulation, one

can accumulate the probability density function (pdf) of the number density,  $p(\rho)$ , in the form of a histogram averaged over many independent samples of  $\rho$ . The form of such a distribution close to liquid-gas coexistence is shown in schematic form in fig. 3.

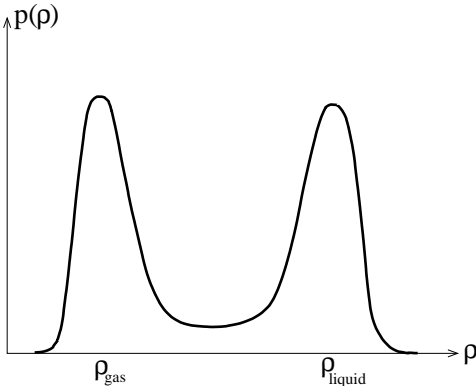


FIG. 3. A schematic diagram of the form of  $p(\rho)$  on the liquid-gas phase boundary.

The principal feature of this distribution is its bimodal (double-peaked) character. Each of the two peaks corresponds to one of the pure phases –the low density peak to the gas phase and the high density peak to the liquid phase. The location of the liquid-gas phase boundary line in the  $\mu - T$  plane is prescribed formally by the equal peak weight criteria i.e. by the set of values of  $\mu$  and  $T$  for which the integrated weights (areas) under the two peaks are equal. Thus to locate liquid-gas coexistence in a simulation one must tune  $\mu$  and  $T$  until the measured form of  $p(\rho)$  is doubly peaked with equal area under each peak. The problem for simulations is that to obtain accurate estimates for the relative peak weights, the simulation procedure must supply bountiful independent samples from each of the two phases, which in turn necessitates that it pass many times back and forth between them.

Unfortunately, the inter-phase route necessarily traverses the mixed-phase configurations in which regions of both phases coexist within the simulation box. Such configurations have, on account of their surface tension, an *a-priori* probability that is intrinsically low compared to those of the pure phase states. This, of course, is the physical origin of the trough separating the two peaks of  $p(\rho)$  which may accordingly be regarded as a “probability (or free energy) barrier” to inter-phase transitions [7]. The height of this barrier is taken to be the ratio of the maximum (peak) value of  $p(\rho)$  to its minimum value in the trough. For large barrier heights, the free energy penalty associated with forming mixed-phase configurations is so high that transitions between the two pure phases can become very rare on the timescale accessible to simulation. As a consequence, the correlation time becomes large, hindering the accumulation of independent statistics on the relative peak weights and thence

the accurate location of the phase boundary.

The barrier height (and hence the scale of the difficult) depends on the temperature. At the critical temperature the surface tension vanishes and with it the probability barrier [8]. If, however, one follows the liquid-gas boundary to progressively lower sub-critical temperatures, thermal fluctuations diminish and the surface tension grows. This is manifest in a growth in the barrier height accompanied by a narrowing of the peaks of  $p(\rho)$ . These features are illustrated in fig. 4 which shows the measured form of  $p(\rho)$  (obtained using the GCE algorithm of box 1.) for the LJF close to the phase boundary for the two temperatures  $T = 0.985T_c$  and  $T = 0.965T_c$ . Also shown in fig. 4(b) is the corresponding evolution of the density expressed as a function of the number of Monte Carlo insertion/deletion attempts. For the higher temperature, the barrier height is approximately 5 and inter-phase transitions are fairly frequent. On decreasing the temperature to  $0.965T_c$ , however, the barrier height increases to a factor 30 and inter-phase crossings become comparatively much rarer. This reluctance to transform between the phases is, of course, none other than the hysteresis phenomenon, viewed not from the standpoint of thermodynamics, but in terms of the underlying statistical mechanics [7].

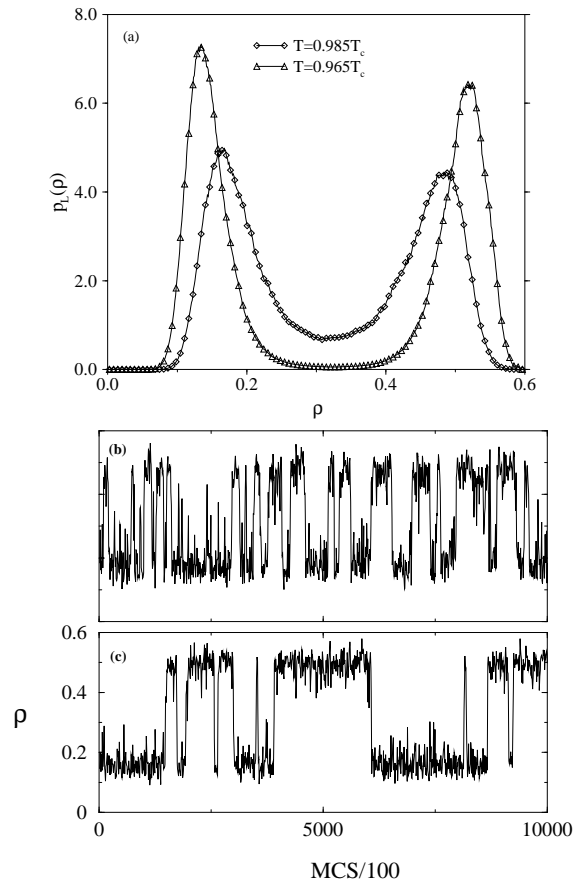


FIG. 4. (a) The form of  $p(\rho)$  at  $T = 0.985T_c$  and  $T = 0.965T_c$  (b) The associated time evolution of the number density at  $T = 0.985T_c$  and (c)  $T = 0.965T_c$

Qualitatively similar effects occur if the linear dimension of the simulation box  $L$  is increased. The barrier height grows because the surface tension of the interface increases proportionally to its area ( $\sim L^2$  for  $d = 3$ ). Additionally, the peaks of  $p(\rho)$  narrow due to ‘self-averaging’ of fluctuations. Even for quite modest system sizes the barrier can be prohibitively large for inter-phase crossings to occur on the accessible simulation timescale.

Effectively then, one is caught between the ‘rock’ of wishing to minimise finite-size effects by employing a large simulation box, and the ‘hard place’ of seeking to sample on timescales exceeding the correlation time. Evidently therefore, a superior approach to bare GCE simulation is called for if one is to tackle the problem of first order phase transitions at temperatures significantly below that of criticality. Indeed, over recent years considerable effort has been invested in developing new MC simulation methods for circumventing the problems identified above. In the next sections we describe one solution to the problem which is rapidly becoming the method of choice for high resolution studies of fluid phase equilibria.

### III. BEATING THE BARRIER

Approaches for dealing with the free energy barrier in simulations of phase transitions fall broadly into two categories

- (i) Simulations without interfaces
- (ii) Biased sampling techniques

Foremost in category (i) are methods such as the Gibbs Ensemble Monte Carlo (GEMC) [9] and Gibbs-Duhem integration [10], both of which have enjoyed widespread use and popularity in studies of phase transitions in model fluids. Although quite distinct in character, both these methods serve to link the pure phases thermodynamically, without traversing mixed-phase configurations. Both are versatile and fairly easy to use. However, they also have significant drawbacks as discussed in Sec. V. Specifically, it seems difficult using the GEMC method to obtain coexistence data of high statistical quality without a large investment of computational effort. By comparison, Gibbs-Duhem integration is more efficient, but potentially suffers from integration errors rendering it difficult to assess the accuracy of results for phase boundary properties.

More recently, an alternative approach has emerged [11] –one which although arguably less straightforward to implement, offers the rewards of considerably greater efficiency, precision and flexibility than GEMC or Gibbs-Duhem integration. This scheme is based on a synthesis of two existing simulation techniques: Multicanonical

biased sampling and Histogram Reweighting. In the remainder of this article, we shall describe how this combined method operates and set out in a step-by-step fashion how one goes about implementing it in practice.

#### A. Multicanonical Sampling

Multicanonical MC owes its origin to the biased sampling techniques first introduced in the 1970’s by Torrie and Valleau to calculate free energies [12]. Latterly however, such techniques have gained fresh impetus with the realisation [13] that they permit the bridging of the free energy barrier at a first order phase boundary. In this context the term ‘‘Multicanonical sampling’’ was coined and the method applied successfully to the study of phase transitions and free energy landscapes in a variety of lattice-based spin systems [14].

The basic idea underpinning Multicanonical MC is to *preweight* the sampling of configuration space in such a way as to artificially enhance the occurrence of the mixed-phase configurations of intrinsically low probability. By so doing it is possible to overcome the probability barrier separating the two pure phases, thereby allowing the simulation to pass unhindered between them. The result is a great reduction in the correlation time of the sampling process.

Within the GCE framework, the biasing is achieved by use of a preweighting function incorporated into the Metropolis acceptance criteria for particle insertions and deletions (cf. Box 1). Its purpose is to modify (with respect to standard Boltzmann statistics) the probability with which configurations of the various densities are visited, in such a way that the measured number density pdf is approximately *flat* over the entire density range separating the two pure phases. Of course the results of such biased simulations deviate from Boltzmann statistics and consequently lack direct physical significance. Nevertheless, it is possible (as we describe below) to *unfold* from the simulation results the unwanted effects of the imposed bias, thence recovering the physically relevant quantities which would have been obtained in an unbiased simulation had sufficient run-time been available. In general, however, there is a price to be paid for this gain, and that is the expenditure of effort involved in finding a suitable form for the preweighting function. Fortunately it transpires that for the purposes of tracing phase boundaries this is not always necessary, it being possible to obtain a suitable preweighting function for ‘free’.

##### 1. Formalism

Let us begin by considering the GCE form of the particle number pdf,  $p(N)$ , at inverse temperature  $\beta = 1/k_B T$  and chemical potential  $\mu$ . For a system of volume  $V$  this

takes the form of a simple average of the Boltzmann factor over all possible particle positions [2]:

$$p(N | V, \beta, \mu) = \frac{1}{Z} \prod_{i=1}^N \left\{ \int_V dr_i \right\} e^{-\beta \mathcal{H}} \quad (3.1)$$

where  $\mathcal{H}$  is the configurational Hamiltonian given by  $\mathcal{H}(\{\mathbf{r}\}, N) \equiv E(\{\mathbf{r}\}) - \mu N$ , while  $Z = Z(\beta, \mu)$  is the partition function which serves to normalise the distribution to unit integrated weight.

The multicanonical method operates by sampling not from a simple Boltzmann distribution with Hamiltonian  $\mathcal{H}(\{\mathbf{r}\}, N)$ , but from a modified distribution with effective Hamiltonian

$$\tilde{\mathcal{H}} = \mathcal{H} + \eta(N) \quad (3.2)$$

where  $\eta(N)$  is a preweighting function defined on the set of particle numbers  $N$  [15]. The associated particle number distribution is given by

$$\tilde{p}(N | V, \beta, \mu, \eta(N)) = \frac{1}{\tilde{Z}} \prod_{i=1}^N \left\{ \int_V dr_i \right\} e^{-\beta \tilde{\mathcal{H}}} \quad (3.3)$$

Let us now suppose for the sake of argument that we are able to choose the preweighting function such that  $\eta(N) = \ln p(N)$  where  $p(N)$  is the desired Boltzmann density distribution. Inspection of eqs. 3.1–3.3 reveals that this implies  $\tilde{p}(N) = \text{constant} \forall N$ . To the extent that such a choice of weight function can actually be realised, the density then performs a 1-d random walk over its entire domain, thereby allowing extremely efficient accumulation of the preweighted histogram  $\tilde{p}(N)$ .

Unfortunately, this happy state of affairs cannot in general be immediately achieved because the preweighting function  $\eta(N) = \ln p(N)$  that serves to flatten  $\tilde{p}(N)$  is, of course, just the logarithm of the function we are trying to find! Means must therefore be found to obtain a form for  $\eta(N)$  that approximates  $\ln p(N)$  sufficiently well that inter-phase transitions occur with an acceptably high frequency. More refined forms for  $\eta(N)$  can thereafter be obtained in the further course of the study.

Let us assume that a suitable preweighting function *has* been found, and a simulation performed to obtain good statistics for  $\tilde{p}(N)$ . The next step is to infer the distribution  $p(N)$  we actually seek by unfolding the effects of the multicanonical preweighting. This is achievable because knowledge of the preweighting function tells us exactly by what degree the relative probabilities of the states of various  $N$  were altered in the simulation with respect to the true Boltzmann statistics. One therefore need only divide out the relative probability enhancements from  $\tilde{p}(N)$  to yield  $p(N)$ . This is done for each value of  $N$  in the range of interest by the simple reweighting:

$$p(N | V, \beta, \mu) = e^{\eta(N)} \tilde{p}(N | \beta, \mu, \eta(N)) \quad (3.4)$$

The details of the practical implementation of this procedure are described in Sec. III C.

## B. Histogram reweighting

Histogram Reweighting is the second ingredient in our simulation procedure. It rests upon the observation that histograms of observables accumulated at one set of model parameters (in our case  $\beta$  and  $\mu$ ) can be analysed to provide estimates of histograms appropriate to other values of these parameters. Consider the *joint* probability distribution of energy and particle number fluctuations at some particular parameter values  $\beta = \beta_0$  and  $\mu = \mu_0$ . Formally this is given by

$$p(N, E | V, \beta_0, \mu_0) = \frac{1}{Z_0} \prod_i^N \left\{ \int_V dr_i \right\} \delta(E - E(\{r_i\})) e^{-\beta_0 \mathcal{H}_0} \quad (3.5)$$

where  $\mathcal{H}_0(\{\mathbf{r}\}, N) \equiv E(\{\mathbf{r}\}) + \mu_0 N$ . It is easy to show [16] that an estimate for the form of  $p(N, E)$  at some other parameters  $\beta = \beta_1, \mu = \mu_1$  can be obtained from the measured pdf by the simple reweighting:

$$p(N, E | V, \beta_1, \mu_1) = \frac{Z_1}{Z_0} e^{-(\beta_1 \mathcal{H}_1 - \beta_0 \mathcal{H}_0)} p(N, E | V, \beta_0, \mu_0) \quad (3.6)$$

where the ratio  $Z_1/Z_0$  is an unimportant constant which is effectively absorbed into the normalisation. If desired, this joint distribution can then be marginalised to yield a uni-variable distribution, eg. the particle number pdf at  $\beta_1, \mu_1$ :

$$p(N | V, \beta_1, \mu_1) = \int dE p(N, E | V, \beta_1, \mu_1) \quad (3.7)$$

Hence, in principle at least, a single simulation at one state point in the phase diagram suffices to obtain information concerning all other state points. Unfortunately the reality of the situation is less auspicious. Owing to finite sampling time, it is not possible *in practice* to reweight a single histogram obtained from a simulation at some  $\beta_0, \mu_0$  to arbitrary values of  $\beta_1, \mu_1$ . Instead the parameters to which one extrapolates must be close (in a sense we shall describe) to those at which the simulation was actually performed, otherwise the procedure loses accuracy.

The problem is traceable to the fact that the reweighting represented by eq. 3.6 may drastically modify the relative statistical weights of the various members of the set of configurations that contribute to the spectrum of measurements. Specifically, difficulties arise with that subset of sampled configurations having very low Boltzmann weight at the simulation parameters  $\beta_0, \mu_0$ , members of which consequently occur only very rarely in the sample. For expectation values of observables calculated at  $\beta_0, \mu_0$ , contributions from this rare subset of configurations do not contribute disproportionately to statistical uncertainties. However, under the reweighting to  $\beta_1, \mu_1$ ,

the configurations in question may be assigned a much greater statistical weight, one which does not reflect their actual representation in the overall sample. This has the effect of magnifying the overall statistical error on measured expectation values and is manifest as a reweighted histogram that appears ‘ragged’ in its extremal regions.

One way of dealing with this problem is to perform a sequence of separate simulations at strategic intervals across the range of model parameters of interest. Typically the intervals are chosen such that histogram of some observable (eg. the energy) accumulated at neighbouring state points in the sequence overlap within some region of their domain. The role of Histogram Reweighting is then to interpolate into the regions of parameter space between the simulation points. In this context it should be noted that it is possible to combine (in a self consistent fashion) the results of a number of different simulations at different model parameters and perform Histogram Reweighting on the *aggregate* data. For a description of this more sophisticated procedure we refer the reader to refs. [16,2].

### C. Stitching together the pieces

So how does one implement the above formalism in a GCE simulation of a fluid? In fact the task falls naturally into two parts: performing the actual multicanonically preweighted simulation and the subsequent data analysis. We consider them in turn.

The business of implementing the multicanonical preweighting within a GCE simulation is basically quite straightforward. Assuming an appropriate set of multicanonical weights has been found, all one need do is read them in and store them in an array. The simulation then proceeds as outlined in Box 1., except that the Metropolis acceptance probabilities for insertion and deletion (eqns. 2.1 and 2.2) are modified to read:

$$p_{\text{acc}}(N \rightarrow N + 1) = \min \left[ 1, \frac{\eta(N)}{\eta(N + 1)} \frac{zV}{(N + 1)} \exp(-\beta(\Delta E^I)) \right] , ; \quad (3.8)$$

$$p_{\text{acc}}(N \rightarrow N - 1) = \min \left[ 1, \frac{\eta(N)}{\eta(N - 1)} \frac{N}{zV} \exp(-\beta(\Delta E^D)) \right] . \quad (3.9)$$

Consider now the simulation quantities we seek to obtain, namely the probability distributions of  $N, E$  and any other observables of interest. Obviously it is tempting to accumulate these distributions in the form of histograms built up in the course of the simulation by simply binning successive measurements into an array. But for continuous variables such as the energy, this strategy necessitates a prior choice for the histogram bin-width. Should a choice be made that subsequently turns out to be unsatisfactory, then one is faced with little alternative

but to repeat the whole simulation. A superior approach, retaining complete information, involves decoupling the data analysis from the simulation by recording the full history of raw data measurements. This data is then postprocessed by a separate analysis program. Although such an approach can make for large simulation output files, it has the overriding advantage of ensuring maximum flexibility in terms of data analysis.

To facilitate the post processing approach, the raw data should be accumulated in the form of a list. Suppose we perform a GCE MC simulation of the LJF at a given  $\beta = \beta_0$  and  $\mu = \mu_0$ , employing some chosen weight function  $\eta(N)$ . As the simulation proceeds we make a succession of measurements (performed at regular spaced intervals of time) of the observables  $E$  and  $N$ , together with any other quantities of interest. Successive measurements of these observables are gathered into a list by appending them to a file, viz:

$$\begin{aligned} & \{E_0, N_0, O_0, \dots\} \\ & \{E_1, N_1, O_1, \dots\} \\ & \{E_2, N_2, O_2, \dots\} \\ & \vdots \\ & \{E_j, N_j, O_j, \dots\} \\ & \vdots \\ & \{E_M, N_M, O_M, \dots\} \end{aligned}$$

where  $j$  indexes the series of  $M + 1$  measurements and  $O$  denotes an observable of interest. The data list is analysed following the actual simulation by a separate post-processing program, the task of which is three fold. Firstly it should remove from the data the unwanted effects of the preweighting in order to recover the desired Boltzmann distributed statistical properties. Secondly, it should output pdf’s of the observables of interest in the form of histograms. Thirdly, it should (if desired) reweight the data to obtain estimates of histograms appropriate to parameter values different from those at which the simulation was performed.

It turns out that the operations of histogram reweighting and bias removal can be accomplished simultaneously because their mathematical structures are very similar. To do this, one simply runs through the data list assigning each entry  $j$  a statistical weight

$$w_j = e^{[-(\beta_1 - \beta_0)E_j + (\beta_1\mu_1 - \beta_0\mu_0)N_j + \eta(N_j)]} , \quad (3.10)$$

where  $\beta_1, \mu_1$  are the parameters to which one wishes to extrapolate. The complete set of  $M + 1$  weights  $w_0, w_1, \dots, w_M$  is then used to construct the reweighted histogram for some measured observable of interest  $O$ :

$$H(O | V, \beta_1, \mu_1) = \sum_{j=0}^M w_j \delta(O - O_j). \quad (3.11)$$

This histogram, once suitably normalised, constitutes a discrete estimate for the probability distribution

$p(O' | V, \beta_1, \mu_1)$ . Implicit in its construction is the specification of the bin-width, which may need to be tuned to strike a balance between resolution and data smoothness. But with the raw list safely stored in a file, this is something that can be done very quickly.

#### IV. TRACING COEXISTENCE CURVES

We now turn to the actual simulation procedure by which a fluid phase boundary can be determined. For illustrative purposes, we shall remain with our prototype example, the liquid-gas transition of the LJF. The essential approach is nevertheless rather general and can be applied to other types of phase transition such as demixing transitions in fluid mixtures.

Clearly one of the key components of our procedure is multicanonical preweighting, use of which generally entails a degree of preliminary effort in order to determine a suitable preweighting function. It transpires, however, that provided one begins tracing the phase boundary from near the critical point which marks its terminus, no additional effort need be expended determining preweighting functions. Instead these can be obtained for ‘free’ by virtue of histogram reweighting as we shall now describe.

One starts off by gauging the approximate location of the critical point from a series of short runs on a small system. This is not time consuming and can be performed interactively at the computer, provided one arranges that the data list (see section III C) is delivered directly to the screen. One starts by nominating a temperature  $T$  and a large negative value of  $\mu$  at which a short simulation is performed without multicanonical preweighting. The fluctuating number density will typically settle down quite rapidly, and its average value can be estimated visually from the data output. One then repeats this procedure for a succession of progressively larger  $\mu$  values. As  $\mu$  is increased, the average particle number will be observed to increase steadily. However on traversing the hysteresis-shifted phase boundary, a sudden jump will occur in the density. If this jump is large, eg. for the LJ fluid, from  $\rho = 0.05$  to  $\rho = 0.6$  (in units of  $\sigma^{-3}$ ), then the temperature is well below the critical temperature and one should increase  $T$  somewhat and begin again. If the jump is somewhat smaller e.g. from  $\rho \simeq 0.2$  to  $\simeq 0.4$ , then one has obtained an estimate for a near-critical point on the phase boundary  $\mu_\sigma(\beta)$ . Of course, if no jump in density is observed at all then the temperature probably exceeds the critical temperature and should be reduced.

One next performs a longer run for some larger system of interest at the estimated near-critical phase boundary point, let us call it  $\mu_\sigma(\beta_0)$ . Since the surface tension and the associated barrier to inter-phase crossings are low near criticality, it should be possible to accumulate an accurate form for  $p(N, E)$  (including information on

states ‘between the peaks’) without resort to multicanonical preweighting. Having done this, the next step is to reweight the data accumulated from this run to obtain an estimate of the form of  $p(N)$  at some lower temperature point on the phase boundary [18]. This is achieved by first choosing an extrapolation temperature  $\beta_1$  inside the range of reliable reweighting (so that the reweighted distribution  $p_{ex}(N | \beta_1, \mu_1)$  appears smooth). One then tunes  $\mu$  within the histogram reweighting scheme until  $p_{ex}(N | \beta_1, \mu_1)$  is bimodal with equal area under each peak. This tuning procedure can be easily automated within the analysis program to deliver precise values of the phase boundary chemical potential  $\mu_1 = \mu_\sigma(\beta_1)$ .

The reweighted phase boundary histogram  $p_{ex}(N | \beta_1, \mu_1)$  will, on account of the lower temperature, be more strongly peaked than that from which it derives. Thus multicanonical preweighting will probably be necessary for a new simulation at  $\beta_1, \mu_1$ . Fortunately however, a suitable preweighting function is already to hand – it is just the extrapolated function  $p_{ex}(N | \beta_1, \mu_1)$ . Thus all one need do is set  $\eta(N) = p_{ex}(N | \beta_1, \mu_1)$  and perform a multicanonical simulation at  $\beta_1, \mu_1$  to obtain the actual distribution  $p(N, E | \beta_1, \mu_1)$ .

One then simply iterates this procedure: histogram reweighting of  $p(N, E | \beta_1, \mu_1)$  is used to estimate a phase boundary point  $\mu_2 = \mu_\sigma(\beta_2)$  at temperature  $\beta_2$ , together with the extrapolated distribution  $p_{ex}(N | \beta_2, \mu_2)$ . The latter serves as a preweighting function for a further simulation at  $\mu_2, \beta_2$ , and so on. In this way one steps down the coexistence curve, obtaining at the same time the locus of the phase boundary  $\mu_\sigma(\beta)$  and the associated set of number density pdf’s. Clearly the maximum feasible step size is set by the range of reliable histogram extrapolation, which does decrease with increasing system size. In practice, however, quite large strides can be made even for large systems. For example, in reference [11], a system of approximately 600 LJ particles was studied and 7 steps were required to reach a subcritical temperature of  $T = 0.85T_c$ .

The results of implementing this procedure for the LJF [11] are depicted in fig. 5. The forms for  $p(N)$  shown have equal weight in each peak and hence lie on the phase boundary. The associated phase diagram  $\mu_\sigma(\beta)$  is shown in figure 6. The values of the coexisting densities can be simply read off from the peak positions in fig. 5(a). The enormity of the probability barrier that multicanonical preweighting allows one to negotiate is revealed by plotting these distributions on a log scale, fig. 5(b).

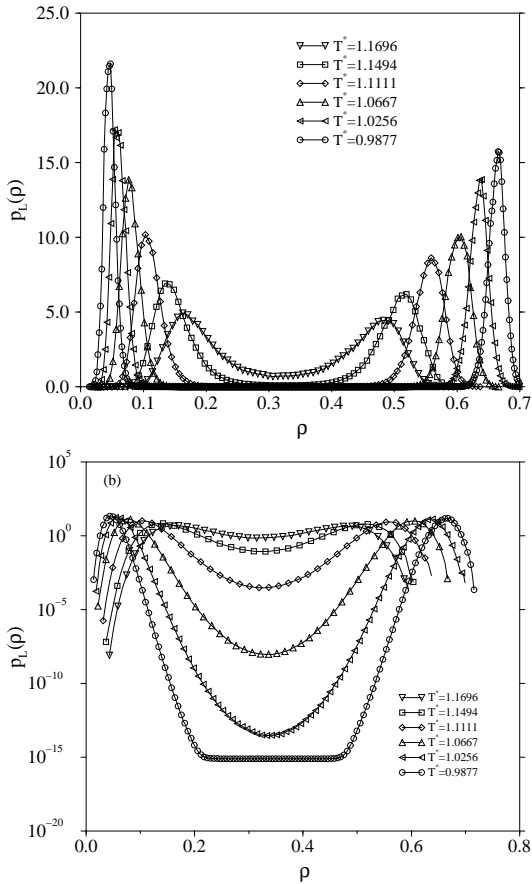


FIG. 5. (a) A selection of the measured forms of  $p(\rho)$  on the phase boundary, for temperatures in the range  $0.95 \leq T \leq T_c$ . (b) The same data expressed on a log scale.

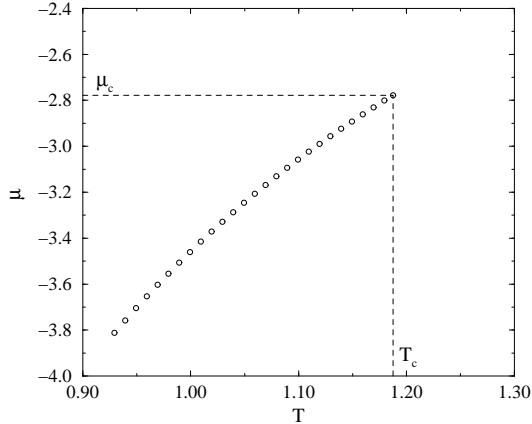


FIG. 6. The line of liquid–vapour phase coexistence in the space of  $\mu$  and  $T$ , for temperatures in the range  $0.95 \leq T \leq T_c$ . Also shown is the location of the critical point [11]

Finally in this section we point out that the measured coexistence form of the density distribution  $p(\rho)$  permits an estimate of the surface tension  $\gamma$ . For a cubic system

of volume  $L^3$ , this is found simply from the ratio of values of  $p(\rho)$  at the peak and at the trough between the peaks [19]:

$$\gamma = \frac{1}{2\beta L^2} \ln \left( \frac{p_{\max}}{p_{\min}} \right)$$

Reference [17] describes a recent application of this relation in a study of the surface tension of the Lennard-Jones fluid.

## V. DISCUSSION AND CONCLUSIONS

To summarise, we have described a scheme whereby information on the locus of a fluid phase boundary is obtainable via the dual mean of multicanonical preweighting and histogram reweighting, married to a standard grand canonical simulation algorithm. The method begins tracing the phase boundary from near the critical point where the free energy barrier to inter-phase transitions is small. Histogram reweighting of the data thus obtained is used to provide an estimate of the location of the phase boundary at some lower temperature, together with a suitable form of the requisite preweighting function. A new multicanonical simulation is performed at this lower temperature phase boundary point and the process is repeated. In this way it is possible to stride down the phase boundary, obtaining pdfs of observables such as the number density from which, in turn, the coexistence properties can be inferred. Such use of multicanonical preweighting completely eliminates hysteresis at first order phase transition.

In cases where one doesn't wish to start tracing a coexistence curve from near the critical point, it is necessary to bootstrap the procedure described above by obtaining an initial phase boundary preweighting function. A variety of techniques exist for achieving this, ranging from simple extrapolation of the weight function into the unsampled region, to more sophisticated analyses of MC transition probabilities. Most of the techniques in common use can be straightforwardly automated. It is beyond the scope of this article to describe these methods in detail, and for further details we refer the interested reader to the literature [20,14].

Although we have illustrated our approach solely in the context of a simple fluid model, it should be noted that it is equally applicable to complex fluids such as molecules or polymers. In these systems, however, the GCE insertion probability is often small, so it is necessary to supplement the standard algorithm with a more intelligent insertion scheme—one which performs a biased choice of a molecular orientation favourable for the insertion. Methods such as Configurational Bias Monte Carlo [21] and Recoil Growth [22] allow one to do this. Apart from this added complication, multicanonical preweighting and histogram reweighting are implemented exactly as for a simple fluid.

The scheme we have described is generalisable to other simulation ensembles such as the constant-NpT ensemble in which density fluctuations occur by means of volume changes at constant particle number, pressure and temperature. Use of this ensemble can be more efficient than the GCE when dealing with very dense fluids where the success rate of particle insertions and deletions is small. The natural variable in which to preweight a constant-NpT ensemble simulation is the fluctuating volume, but otherwise the formalism is very similar to that described above. For other types of phase transitions, such as the liquid-liquid transitions occurring in binary fluid mixtures, a suitable variable in which to preweight is usually the order parameter for the transition eg. the concentration of one species.

It is instructive to compare the scheme described in this article with other commonly used methods for tracing phase boundaries. One such method is the Gibbs-Duhem integration method wherein pairs of single phase simulations (one for each phase) are performed at various state points along the phase boundary. The single phase results are connected thermodynamically, not by negotiating the free energy barrier at each state point, but via a phase space path that runs back along each side of the phase boundary to some independently-known reference point on the phase boundary. Successive simulation state points along the phase boundary are found from an integration scheme which turns out [23] to be a low order approximation to the histogram reweighting method. The Gibbs-Duhem method is versatile provided one has prior knowledge of a phase boundary reference point and is, for the purposes of obtaining a rough estimate of the phase boundary locus, doubtless faster than the method described in this article. However, its accuracy rests heavily upon the precision with which the boundary reference point is known. Moreover, as one departs from this point, integration errors can grow and provided one remains within the (rather wide) region of metastability bordering either side of the phase boundary line, there is no feedback to indicate that one has in fact strayed away from it. By contrast, the multicanonical method is self-correcting because it reconnects the two phases at each successive simulation state point on the phase boundary.

Another widely used technique is the Gibbs Ensemble MC Method [9]. Two separate simulation boxes (one for each pure phase) are connected thermodynamically by the dual means of particle transfers between the boxes and fluctuations in the box volumes implemented such that the overall volume of the two boxes remains constant. Like Gibbs-Duhem integration, GEMC is very useful for obtaining rough estimates of phase boundaries. The method is free of integration errors since the phases remain directly linked at each phase boundary state point. However, measurements of the pressure and chemical potential must be obtained by a sampling scheme since neither is imposed in the simulation. Moreover, direct comparisons have shown GEMC to be much

less efficient than the methods described in this article because of the computational complexity associated with implementing volume fluctuations [24,25]. Worries have also recently been voiced that the GEMC method suffers more severely from finite size effects than does the GCE [26].

Finally, it should be pointed out that despite their utility in dealing with phase equilibria involving fluids, the specific multicanonical techniques we have described do not permit one to tackle phase transitions involving solids. The problem here is that when attempting to traverse mixed-phase states involving crystalline order, the simulation invariably gets caught in ‘non-ergodic traps’ identifiable with defective crystalline configurations. Recently, however, a new technique has been developed that circumvents this problem by linking the two coexisting phases *without* traversing mixed-phase states. Essentially the method can be thought of as leaping directly from the configuration space of one pure phase to that of the other. Again use of multicanonical sampling is necessary, but this time its role is to encourage the simulation to visit a subset of configurations (in each pure phase) from which a leap to the other phase will be accepted. This new method has recently shown its worth in studies of solid-phase free energy differences and hard sphere freezing [27,28].

## VI. SUGGESTIONS FOR FURTHER STUDY

The following set of problems will help to reader to become more familiar with the techniques described in this article.

1. Using Box 1. as a guide, write a simple Grand Canonical ensemble MC program to simulate the Lennard-Jones fluid with potential cut-off at  $r_c = 2.5\sigma$ . Do not correct for the potential truncation. Make sure the program prints out the particle number and the energy in list form (cf. sec. III C). Further programming details can be found in ref. [2].
2. Run the program at the near critical phase boundary parameters [11]  $\beta\epsilon = 1.1876$ ,  $\beta\mu = -2.778$ , saving the output data list to a file.
3. Write a post-processing program to construct the number density histogram  $p(N)$  from the raw data list.
4. Modify your GCE acceptance probabilities to cater for multicanonical preweighting (cf. secs. III A and III C). Use your measured  $p(N)$  as the preweighting function for a multicanonical simulation at the same  $\beta, \mu$  used in (2) above. Hint: At the extrema of small (large)  $N$ , there will be histogram bins in  $p(N)$  having zero entries. Before using  $p(N)$  as your preweighting function, set these entries to be a constant equal to the smallest non zero entry. This

avoids possible division by zero in the acceptance probabilities.

5. Extend your post-processing program to unfold the effects of the preweighting (as described in Secs. III A and III C) in order to find  $p(N)$ . Check that the form of  $p(N)$  thus obtained agrees with that found without multicanonical preweighting. Compare the correlation time for the sampling processes with and without multicanonical preweighting.
6. Further extend your post-processing program to implement histogram reweighting (as described in Sec. III B and III C). Extrapolate the data obtained at the critical temperature  $\beta\epsilon = 1.1876$  to find the location of the phase boundary and the form of  $p(N)$  at  $\beta\epsilon = 1.17$ . Use this extrapolation as a preweighting function in a new multicanonical simulation at the new phase boundary state point. Compare your results with those of ref. [11]

---

[1] A comparison of the model's phase behaviour with the results of experiment can be useful in helping to refine the model parameters.

[2] D. Frenkel and B. Smit; *Understanding Molecular Simulation*, Academic Press, Boston (1996). See also [http://molsim.chem.uva.nl/frenkel\\_smit](http://molsim.chem.uva.nl/frenkel_smit)

[3] M.P. Allen and D.J. Tildesley; *Computer simulation of liquids* Oxford University Press (1987).

[4] H. Gould and J. Tobochnik; *Introduction to Computer Simulation Methods*, Addison-Wesley, (1996). See also <http://www.kzoo.edu/sip>

[5] D.P. Landau and K. Binder; *A Guide to Monte Carlo Simulation in Statistical Physics*, Cambridge University Press (2000).

[6] See eg. M. Plischke and B. Bergersen; *Equilibrium Statistical Physics*, World Scientific, Singapore (1994).

[7] It can be shown that the constrained free energy  $F(\rho)$  is directly related to the density pdf by  $F(\rho) = -\ln p(\rho)$ . This relation serves to link the thermodynamical interpretation of phase stability in which a system occupies the state of minimum free energy, with the statistical mechanics viewpoint that it is most likely to be found in a state of maximum *a-priori* probability.

[8] The critical point is characterised by strong fluctuations in the density which present distinctive challenges for simulation and theory alike. For an introduction to some of the main issues, see chapter 5 of ref. [6] and also ref. [11].

[9] A.Z. Panagiotopoulos; *Mol. Phys.* **61**, 813 (1987).

[10] D.A. Kofke; *J. Chem. Phys.* **98**, 4149 (1993).

[11] N.B. Wilding; *Phys. Rev.* **E52**, 602 (1995).

[12] G.M. Torrie, J.P. Valleau; *J. Comp. Phys.* **23**, 187 (1977).

[13] B.A. Berg and T. Neuhaus; *Phys. Rev. Lett.* **68**, 9 (1992).

[14] J. E. Gubernatis and N. Hatano; *Computing in Science and Engineering* **2**, 95 (2000).

[15] In fact it is possible to preweight with respect to any system observable, although for the problem of fluid phase transitions the number density is usually the most computationally appropriate quantity.

[16] A.M. Ferrenberg and R.H. Swendsen, *Phys. Rev. Lett.* **61**, 2635 (1988); *ibid* **63**, 1195 (1989); A.M. Ferrenberg and R.H. Swendsen, *Computers in Physics*, **3**(5), 101 (1989).

[17] J. Potoff and A. Z. Panagiotopoulos, *J. Chem. Phys.* **112**, 6411 (2000).

[18] One can also extrapolate to slightly higher temperatures in order to pinpoint the critical point. Special 'finite-size scaling' techniques are required here, as described in detail in reference [11].

[19] K. Binder, *Phys. Rev.* **A25** 1699 (1982).

[20] G.R. Smith and A.D. Bruce, *J. Phys.* **A28**, 6623 (1995).

[21] D. Frenkel and B. Smit, *Computers in Physics* **111**, 246 (1997).

[22] S. Consta, N.B. Wilding, D. Frenkel and Z. Alexandrowicz; *J. Chem. Phys.* **110**, 3220 (1999).

[23] F.A. Escobedo; *J. Chem. Phys.* **113** 8444 (2000).

[24] J.J. Potoff, J.R. Errington and A.Z. Panagiotopoulos; *Mol. Phys.* **97** 1073 (1999).

[25] A.Z. Panagiotopoulos; *J. Phys. Condens. Matter* **12**, R25 (2000).

[26] J.P. Valleau; *J. Chem. Phys.* **108**, 2962 (1998).

[27] A.D. Bruce, N.B. Wilding, G.J. Ackland, *Phys. Rev. Lett.* **79**, 3002 (1997).

[28] N.B. Wilding and A.D. Bruce; *Phys. Rev. Lett.* **85**, 5138 (2000).